Obrabotka metallov (tekhnologiya, oborudovanie, instrumenty) = Metal Working and Material Science. 2026 vol. 28 no. 3 pp. 58–69
ISSN: 1994-6309 (print) / 2541-819X (online)
DOI: 10.17212/1994-6309-2026-28.3-58-69

NSTU NETI

Obrabotka metallov - Metal Working and Material Science

Journal homepage: http://journals.nstu.ru/obrabotka_metallov

Investigation of temperature during machining of titanium nickelide TN-1

Nikolaj Bobrovskij [1, a], *Anton Kisel'* [1, 2, b, *], *Renat Kamenov* [1, 2, c], *Dmitrij Podashev* [3, d], *Pavel Tselikov* [3, e], *Kajnikayat Kisel'* [2, 3, f]

[1] National Research University "MIET", 1 Shokin Square, Moscow, Zelenograd, 124498, Russian Federation
[2] Togliatti State University, 14 Belorusskaya Str, Togliatti, 445020, Russian Federation
[3] Kaliningrad State Technical University, 1 Sovetsky Avenue, Kaliningrad, 236022, Russian Federation

[a] https://orcid.org/0000-0002-9299-2822, bobrnm@yandex.ru; [b] https://orcid.org/0000-0002-8014-0550, kisel1988@mail.ru;
[c] https://orcid.org/0000-0001-9181-5704, renatkamenov@mail.ru; [d] https://orcid.org/0000-0001-9112-9253, dmitrij.podashev@klgtu.ru;
[e] https://orcid.org/0009-0008-6040-0600, patersort@list.ru; [f] https://orcid.org/0009-0003-2113-2192, k.kisel-ks@yandex.ru

ARTICLE INFO

Article history:
Received: 05 March 2026
Revised: 30 May 2026
Accepted: 11 July 2026
Available online: 15 September 2026

Keywords:
Mechanical machining
Titanium nickelide (nitinol)
Cutting temperature
Thermal imager
Machining mode
Cutting speed
Feed
Depth of cut
Technological heredity
Surface plastic deformation

Funding
The research was supported by a grant from the Russian Science Foundation, project No. 22-19-00298-P, https://rscf.ru/en/project/22-19-00298/.

ABSTRACT

Introduction. The temperature generated in the machining zone is a critical parameter that affects the dimensional accuracy, surface quality, material properties of the workpiece, and tool wear resistance. This is especially important when machining critical components for machinery operating under severe conditions. Such parts are typically made from heat-resistant alloys, with titanium nickelide (nitinol) being a notable example. Temperature can be influenced by various methods, but the primary approach used in this study was the selection of rational machining parameters. ***The purpose of this work*** is to evaluate the impact of cutting parameters on the temperature generated during the machining of titanium nickelide workpieces. **Materials and methods.** Experimental studies were conducted on the turning of titanium nickelide (*TN-1*) workpieces. The variable parameters in the tests were the cutting parameters: cutting speed ***V*** (m/min), feed rate ***S*** (mm/rev), and depth of cut ***t*** (mm). The temperature ***T*** (°C) generated during machining was measured using a *CEM DT-9897* thermal imager. The machining process was recorded during the tests, and was later reviewed to determine the peak cutting temperature. This value was taken as the average cutting temperature, as its maximum occurs at the contact point between the chip and the workpiece's front surface, which is obscured from direct observation by the chip itself. **Results and discussion.** The following results are obtained during the research: experimental studies are conducted according to a developed plan, and the cutting temperature generated under various turning modes of *TN-1* titanium nickelide workpieces are determined; mathematical dependencies of temperature on cutting parameters are established; verification of the obtained dependencies is performed by comparing calculated cutting temperatures with experimental data (it is found that, according to the derived dependencies, the calculation error does not exceed 5.8%); rational turning modes for titanium nickelide workpieces are established based on cutting temperature, and recommendations for selecting cutting parameters for finish and semi-finish machining are developed.

For citation: Bobrovskij N.M., Kisel' A.G., Kamenov R.U., Podashev D.B., Tselikov P.V., Kisel' K.Kh. Investigation of temperature during machining of titanium nickelide TN-1. *Obrabotka metallov (tekhnologiya, oborudovanie, instrumenty) = Metal Working and Material Science*, 2026, vol. 28, no. 3, pp. 58–69. DOI: 10.17212/1994-6309-2026-28.3-58-69. (In Russian).

Introduction

Components for machinery operating under severe service conditions are manufactured from materials with high mechanical and technological properties. Such machinery includes aircraft, aerospace, mining, and related equipment. Critical components are often made from difficult-to-machine heat-resistant alloys containing nickel and titanium. In this case, machining is accompanied by high forces and temperatures

*** Corresponding author**
Kisel' Anton G., Ph. D. (Engineering), Associate Professor, Senior Researcher
Togliatti State University,
14 Belorusskaya St.,
445020, Togliatti, Russia
Tel.: +7 999 458-08-25, **e-mail:** kisel1988@mail.ru

acting on the tool and the workpiece, which adversely affects dimensional accuracy, surface quality, workpiece material properties, and tool wear resistance [1–5]. Ultimately, these increase reject rates, tool consumption, and overall production cost. Several approaches can reduce these negative factors, and the first is the selection of rational machining parameters. In many studies, the temperature generated in the machining zone is used as the controlled parameter when determining rational modes, since temperature affects all the above-mentioned characteristics of the tool and the finished part.

Several methods are used to determine temperature in the machining zone:

– machining simulation using *CAE* systems [1, 2, 6–8];

– use of artificial, semi-artificial, or natural thermocouples [2, 3, 6, 7, 9–12];

– calculation using physical or empirical relationships [4, 9, 13, 14];

– measurement of infrared radiation using pyrometers or thermal imagers [4, 11, 15–20].

Each method has advantages and limitations. Non-contact methods are becoming increasingly common because they are versatile, enable remote real-time assessment of temperature distribution in the observed area, and are easy to use. For these reasons, measurements in this study were performed using a thermal imager.

An example of difficult-to-machine alloys used in aircraft, aerospace, and other machinery is titanium nickelide, also known as nitinol [21–23]. A distinctive feature of this alloy is the shape memory effect: the ability to recover its shape after preliminary cold deformation when temperature or other conditions change [24, 25].

The literature contains some recommendations for machining workpieces made from this class of alloys and some patterns in quality indicators under different modes; however, such publications are scarce and do not fully characterize the processes involved.

In particular, reference [26] compares conventional cutting of nitinol workpieces with laser machining, electrical discharge machining, chemical machining, and micromachining. It assesses the influence of machining parameters and cutting fluid on burr formation, surface properties, and phase-transition temperature. The study shows that material removal during micromachining requires less energy and generates less heat, making it possible to use higher process parameters, namely feed and cutting speed.

Reference [27] presents research on the dependence of material removal rate, tool life, and surface roughness on spindle speed, feed, and depth of cut during turning of a nitinol workpiece. Optimal machining parameters were identified to minimize negative factors.

Reference [28] considers different mathematical descriptions of the relationship between cutting force and surface roughness, on the one hand, and process parameters and laser power, on the other, during laser-assisted turning of nitinol workpieces. The adaptive neuro-fuzzy inference system (*ANFIS*) provided the highest prediction accuracy. Cutting speed was found to be the main factor determining the generated cutting force and the resulting surface roughness.

Reference [29] reports the influence of turning parameters for a nitinol workpiece on material removal rate, tool wear, and surface roughness. An optimal machining mode was established to achieve the best performance for these indicators.

Reference [30] is a review article on high-speed micromilling of nitinol workpieces. It discusses machining problems and possible directions for further research: promising tool materials, alternatives to cutting processes, mode optimization methods, post-processing techniques, and environmental effects.

Reference [31] examines the effect of machining modes on material removal rate and surface roughness of a nitinol workpiece during wire electrical discharge machining. It concludes that the *ANFIS* model provides more accurate prediction of electrical discharge machining responses. At the same time, implementation of *ANFIS* can be complex and require substantial computational resources.

No scientific sources were found that reported the temperature generated during mechanical machining of nitinol. Therefore, ***the aim of this study*** is to evaluate the influence of cutting parameters on the temperature generated during machining of titanium nickelide workpieces. To achieve this aim, ***the following tasks*** were set:

– to perform experimental studies to determine the cutting temperature generated under different modes;

– to establish mathematical relationships between temperature and cutting parameters;

– to verify the obtained relationships by comparing calculated cutting temperatures with experimental data;

– to establish rational modes for machining titanium nickelide based on cutting temperature and develop recommendations for selecting cutting parameters.

Methods

Since turning is one of the most widely used machining processes, it was selected for the study. The experiments were performed on a *UTS6* desktop *CNC* lathe.

TN-1 alloy was used as the workpiece material because it is one of the common shape memory alloys used in mechanical engineering. Its main chemical components are nickel (53.5–56.5 wt.%) and titanium (42.2–45.2 wt.%). A coupling for thermomechanical joining of tubes is an example of a *TN-1* product (Fig. 1). The workpieces used in the experiments had a diameter of 10 mm.

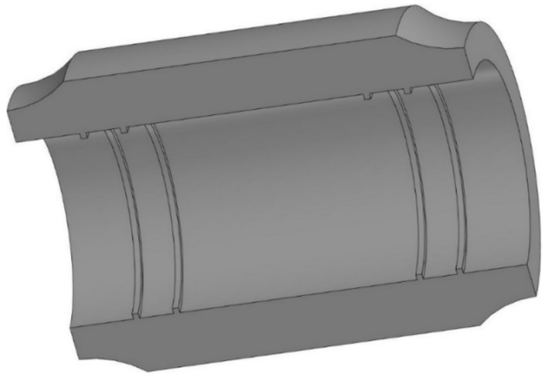

Fig. 1. Coupling for thermomechanical joining of shape memory alloy tubes (sectional view)

The cutting tool used was a *CCMT09T308-EM* turning tool with an indexable carbide insert coated with an *AlTiN*-based *PVD* coating.

The varied cutting parameters were cutting speed ***V*** (m/min), feed rate ***S*** (mm/rev), and depth of cut ***t*** (mm). To evaluate the behavior of the response function, one point was added to the center of the design for each depth of cut. The modes used in the study are similar to those used at mechanical engineering enterprises (Table 1).

The temperature ***T*** (°C) generated during machining was measured using a *CEM DT-9897* thermal imager (Fig. 2).

The temperature measurement range of this thermal imager is –20 to +650 °C. According to the specifications, the measurement error is ±2%. The emissivity coefficient **ε** is adjustable, which makes

Table 1

Experiments plan

Exp. No.	***V*** (m/min)	***S*** (mm/rev)	***t*** (mm)
1	5	0.03	0.1
2	30	0.03	0.1
3	5	0.2	0.1
4	30	0.2	0.1
5	5	0.03	0.3
6	30	0.03	0.3
7	5	0.2	0.3
8	30	0.2	0.3
9	17.5	0.115	0.1
10	17.5	0.115	0.3

Fig. 2. Thermal imager *CEM DT-9897*

it possible to set it according to the characteristics of the observed surface. An assessment of open-source data showed that **ε** for polished or highly reflective surfaces of various alloys may range from 0.1 to 0.3. A calibration experiment refined this value, and **ε** = 0.19 was established for the studied material, which corresponds to unoxidized nickel alloys. The temperature ***T*** (°C) was measured from a distance of 500 mm from the machining zone. The thermal imager was directed at the cutting zone at an angle of 30–35° so that the working part of the tool, the machined workpiece, and part of the three-jaw chuck were captured. Cutting fluid was not supplied to the cutting zone, in accordance with industrial practice and to reduce the number of influencing factors.

Because the observed process was not steady-state, with the chip separating from the workpiece and moving unpredictably, an additional observation error was introduced. As a result, the temperature first increased and then fluctuated downward around a certain steady value. Therefore, the process was video recorded, and after the experiment the video was reviewed; the highest cutting temperature was recorded as the observation result. This value was taken as the average cutting temperature because the maximum occurs at the contact between the chip and the rake face, which is hidden from direct observation by the chip.

Each experiment was performed as follows. On the machine, the tool with an unworn cutting insert was brought to the initial position. Video recording on the thermal imager was switched on. The machine was started according to the program with the required cutting parameters. After machining was completed, the machine was stopped and video recording was switched off. The used cutting insert was removed and replaced with a new one. The procedure was then repeated for each machining mode considered. The resulting videos were reviewed to determine the maximum temperature, which was recorded in the table.

An example of an image obtained during the tests is shown in Fig. 3.

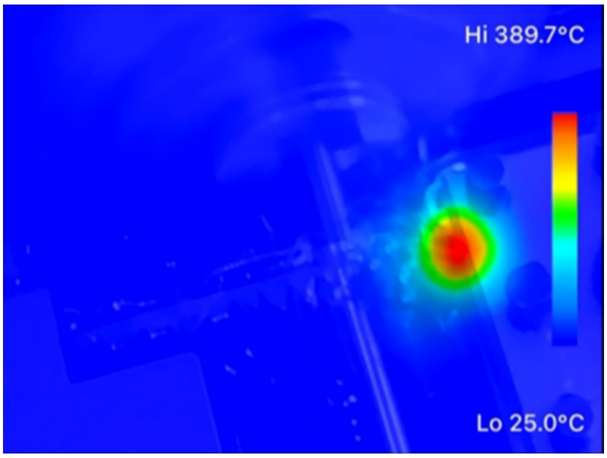

Fig. 3. Example of an image obtained with a thermal imager

Results and discussion

The measured cutting temperatures ***T*** are presented in Table 2.

The table shows that at a small depth of cut (***t*** = 0.1 mm), increasing the feed from 0.03 to 0.2 mm/rev increases the temperature by a factor of 1.29–2.29. This difference is explained by the fact that at low feed, bulk plastic deformation and heat accumulation near the tool dominate (low temperature in the cutting zone, but deep heating). As feed increases, intensive chip removal occurs and the main heat generation shifts into the volume of the removed layer (high temperature in the cutting zone, but more uniform distribution). In addition, the factor of phase transformations (austenite/martensite) may amplify this effect.

Since the literature does not report studies on temperature measurement during turning of this alloy, it was not possible to compare the obtained data with earlier results from other researchers. However, many results are available for machining nickel-based heat-resistant alloys such as *Inconel 718* [32]. According to the data presented in that publication, when this alloy is machined at a cutting speed of 30 m/min, a feed of 0.2 mm/tooth, and a depth of cut of 0.25 mm, the average cutting temperature is about 283 °C. Under comparable cutting conditions for *TN-1* alloy, the temperature was 440.5 °C (Table 2). Thus, when machining nitinol, the temperature generated in the cutting zone is noticeably higher, which can be explained by the lower thermal conductivity of this alloy compared with *Inconel 718*.

Table 2

Experimental results

Exp. No.	***V*** (m/min)	***S*** (mm/rev)	***t*** (mm)	***T*** (°C)
1	5	0.03	0.1	183.4
2	30	0.03	0.1	356.2
3	5	0.2	0.1	420.1
4	30	0.2	0.1	459.2
5	5	0.03	0.3	290.0
6	30	0.03	0.3	389.7
7	5	0.2	0.3	303.8
8	30	0.2	0.3	440.5
9	17.5	0.115	0.1	139.2
10	17.5	0.115	0.3	215.4

The dependence of the generated temperature on cutting parameters was determined by two methods in order to select the more accurate one.

The first method used the *Box-Cox* transformation. According to this method, the variable values were coded using the following expressions:

$$V_c = \frac{V - 17.5}{12.5}, \quad S_c = \frac{S - 0.115}{0.085}, \quad t_c = \frac{t - 0.2}{0.1}, \tag{1}$$

where $\boldsymbol{V_c}$, $\boldsymbol{S_c}$, and $\boldsymbol{t_c}$ are the coded values of cutting speed, feed, and depth of cut, respectively.

The proposed method was implemented using the *Python* programming language. As a result of the corresponding transformations, the following formula was obtained in terms of coded variables:

$$\tilde{T} = 480.6509 + 214.4369V_c + 194.7511S_c + 23.0559t_c + 327.5388V_c^2 +$$

$$+327.5388S_c^2 - 130.4228S_c t_c. \tag{2}$$

The conversion from the coded values obtained via formula (2) is performed using the following expression:

$$T = (1 + 1.2319\tilde{T})^{1/1.2319}. \tag{3}$$

The second method was implemented using the *Statistica* software package, which enables the derivation of functional relationships for two variables and the construction of response-surface plots. Since only two parameters were varied in this study, two separate relationships were obtained – one for each depth of cut. The resulting formulas are presented below:

– for a depth of cut $\boldsymbol{t}$ = 0.1 mm:

$$T = 304.5154 - 16.3046V - 1806.1027S + 0,6838V^2 - 31.4588VS + 14283.737S^2; \tag{4}$$

– for a depth of cut $\boldsymbol{t}$ = 0.3 mm:

$$T = 398.7812 - 9.9281V - 2412.8143S + 0.3812V^2 + 8.7059VS + 10569.7809S^2. \quad (5)$$

The response surfaces for both methods are presented in Figs. 4 and 5.

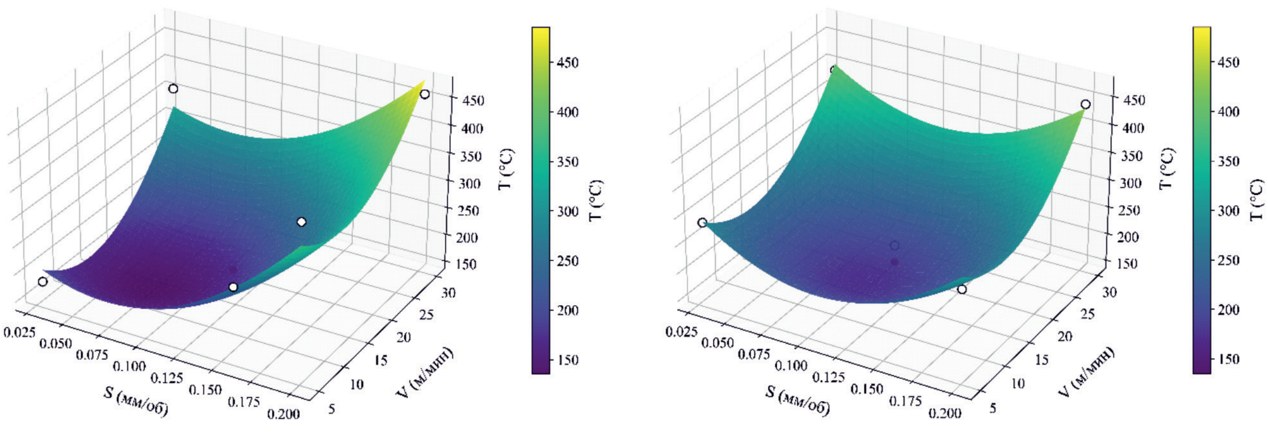

Fig. 4. Dependencies plotted using the Box-Cox transformation:
a – at t = 0.1 mm; *b* – at t = 0.3 mm

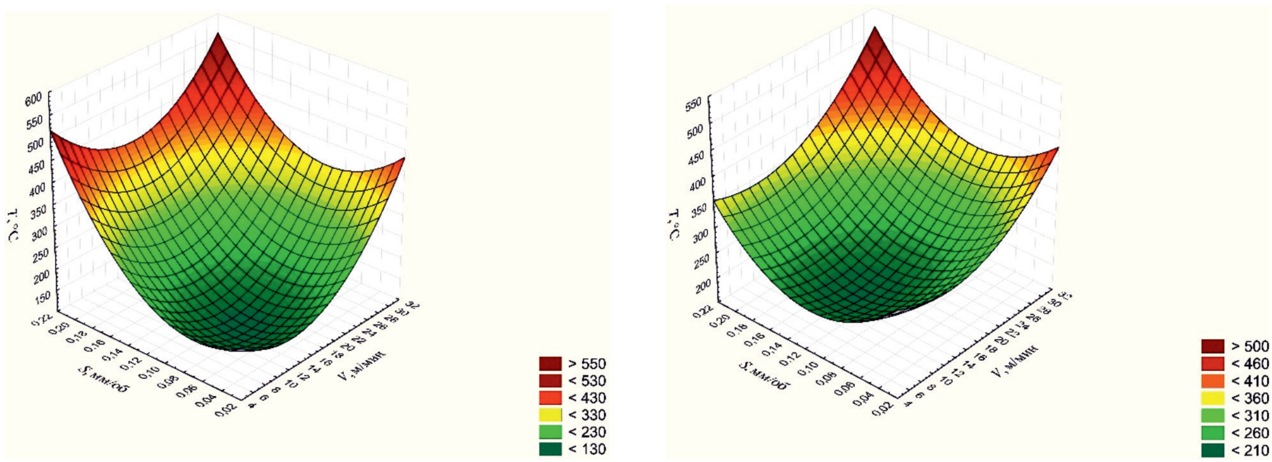

Fig. 5. Dependencies plotted using Statistica software:
a – at t = 0.1 mm; *b* – at t = 0.3 mm

To assess the adequacy of the obtained relationships (2)–(5), the cutting parameters were substituted into the equations, and the resulting calculated values were compared with the experimental data given in Table 3.

To evaluate the accuracy of the calculations performed using the derived relationships, the relative error **ε** (%) was computed; the results are summarized in Table 3. As can be seen from the table, the relationship obtained via the *Statistica* software exhibits higher accuracy, with a maximum error of 5.8%. The considerable discrepancy between the two sets of calculated results may be attributed to the differing approximation approaches employed by the two methods.

The *Box-Cox* transformation is intended to render the response distribution more normal and to stabilize variance. After this transformation, the model is constructed on the corrected data. In contrast, *Statistica* builds a mathematical model that directly approximates the response surface as a function of two variables, selecting coefficients for the individual terms so as to achieve the most accurate description of the experimental data. For this reason, formulas (4) and (5) were adopted for all subsequent calculations.

Table 3

Evaluation of the adequacy of derived dependencies

Exp. No.	***V*** (m/min)	***S*** (mm/rev)	***t*** (mm)	***T*** (°C) (exp.)	***T*** (°C) (*Box-Cox*)	ε (%) (*Box-Cox*)	***T*** (°C) (*Statistica*)	ε (%) (*Statistica*)
1	5	0.03	0.1	183.4	205.6	12.1	194.0	5.8
2	30	0.03	0.1	356.2	323.4	–9.2	361.1	1.4
3	5	0.2	0.1	420.1	380.3	–9.5	418.8	–0.3
4	30	0.2	0.1	459.2	485.3	5.7	452.2	–1.5
5	5	0.03	0.3	290.0	291.1	0.4	297.1	2.4
6	30	0.03	0.3	389.7	401.7	3.1	389.0	–0.2
7	5	0.2	0.3	303.8	325.2	7.0	307.6	1.3
8	30	0.2	0.3	440.5	433.4	–1.6	436.5	–0.9
9	17.5	0.115	0.1	139.2	171.3	23.1	146.5	5.2
10	17.5	0.115	0.3	215.4	185.2	–14.0	221.6	2.9

Inspection of Figs. 5, *a*, *b* reveals that both response surfaces exhibit a minimum point. It is therefore advisable to determine the cutting parameters corresponding to the minimum cutting temperature. To this end, expressions (4) and (5) were differentiated with respect to ***V*** and ***S***, and the resulting derivatives were set equal to zero. Solving the resulting systems of equations yielded the optimal values of cutting speed and feed rate.

It was established that for a depth of cut ***t*** = 0.1 mm, the minimum cutting temperature of 121.89 °C is achieved at a cutting speed ***V*** = 13.72 m/min and a feed rate ***S*** = 0.08 mm/rev. For a depth of cut ***t*** = 0.3 mm, the minimum cutting temperature of 140.08 °C corresponds to ***V*** = 11.77 m/min and ***S*** = 0.11 mm/rev.

Accordingly, the recommended turning parameters for TN-1 titanium nickelide workpieces, based on the criterion of minimum cutting temperature, are as follows:

– at a depth of cut ***t*** = 0.1 mm (finish machining):

$$V = 13.72 \text{ m/min}, \quad S = 0.08 \text{ mm/rev};$$

– at a depth of cut ***t*** = 0.3 mm (semi-finish machining):

$$V = 11.77 \text{ m/min}, \quad S = 0.11 \text{ mm/rev}.$$

The occurrence of a minimum point in the vicinity of the experimental design center is attributed to austenite-to-martensite phase transformations in the workpiece material. Specifically, when machining takes place within the martensitic transformation interval, part of the mechanical energy is expended on the phase transition rather than on thermal dissipation, thereby producing a local decrease in cutting temperature.

Conclusion

The study investigated the influence of cutting parameters on the temperature in the machining zone during turning of *TN-1* titanium nickelide workpieces. In achieving the stated purpose, mathematical relationships were established that make it possible to calculate the cutting temperature for specified process parameters within the applied ranges: cutting speed from 5 to 30 m/min, feed from 0.03 to 0.2 mm/rev, and depth of cut from 0.1 to 0.3 mm. The calculation error does not exceed 5.8%. In addition, temperature-based rational cutting modes were established and recommendations were developed for selecting parameters for finish and semi-finish machining.

The results make it possible to assign cutting parameters according to the temperature in the machining zone, thereby controlling tool wear processes and the changes occurring in the material during heating.

It should also be noted that machined workpieces exhibit technological heredity: their properties, such as structure and texture, change after any processing operation, which in turn affects subsequent stages of part manufacture. Therefore, the results obtained in this study should be taken into account when finishing operations such as surface plastic deformation (*SPD*) are required. Since mathematical relationships describing the patterns of temperature change have been established, they can be used to predict possible material changes and, with certain assumptions, extrapolate these values to other types of processing.

References

1. D'Addona D., Raykar S. Thermal modeling of tool temperature distribution during high pressure coolant assisted turning of Inconel 718. *Materials*, 2019, vol. 12 (3), pp. 408. DOI: 10.3390/ma12030408.

2. Liu H., Meurer M., Bergs T. Modeling and monitoring of the tool temperature during continuous and interrupted turning with cutting fluid. *Metals*, 2024, vol. 14 (11), p. 1292. DOI: 10.3390/met14111292.

3. Liu S., An L., Li H., Fu X., Ju B.-F., Chen Y.-L. Characterization and optimization of a locally boron-doped diamond tool for self-sensing of cutting temperature. *Nanomanufacturing and Metrology*, 2024, vol. 7 (1), p. 24. DOI: 10.1007/s41871-024-00243-8.

4. Díaz-Álvarez J., Tapetado A., Vázquez C., Miguélez H. Temperature measurement and numerical prediction in machining Inconel 718. *Sensors*, 2017, vol. 17 (7), p. 1531. DOI: 10.3390/s17071531.

5. Lakshmanan S., Pradeep Kumar M., Dhananchezian M. Optimization of turning parameter on surface roughness, cutting force and temperature through TOPSIS. *Materials Today: Proceedings*, 2023, vol. 72, pp. 2231–2237. DOI: 10.1016/j.matpr.2022.09.209.

6. Kus A., Isik Y., Cakir M.C., Coşkun S., Özdemir K. Thermocouple and infrared sensor-based measurement of temperature distribution in metal cutting. *Sensors*, 2015, vol. 15 (1), pp. 1274–1291. DOI: 10.3390/s150101274.

7. Ramme J., Wegert R., Guski V., Schmauder S., Moehring H.-C. Development of a multi-sensor concept for real-time temperature measurement at the cutting insert of a single-lip deep hole drilling tool. *Applied Sciences*, 2022, vol. 12 (14), p. 7095. DOI: 10.3390/app12147095.

8. Li G., Lu W., Huang S., Zhang X., Ding S. Analysis and prediction of residual stresses based on cutting temperature and cutting force in rough turning of Ti–6Al–4V. *Heliyon*, 2022, vol. 8 (11), p. e11661. DOI: 10.1016/j.heliyon.2022.e11661.

9. Lapshin V.P., Rusanovsky R.V., Turkin I.A. Evaluation of the influence of the reaction rate of the thermodynamic subsystem on the dynamics of the cutting process in metalworking. *Obrabotka metallov (tekhnologiya, oborudovanie, instrumenty) = Metal Working and Material Science*, 2021, vol. 23, no. 2, pp. 17–30. DOI: 10.17212/1994-6309-2021-23.2-17-30. (In Russian).

10. Patil N.G., Saraf A.R., Kulkarni A.P Semi empirical modeling of cutting temperature and surface roughness in turning of engineering materials with TiAlN coated carbide tool. *Obrabotka metallov (tekhnologiya, oborudovanie, instrumenty) = Metal Working and Material Science*, 2024, vol. 26, no. 1, pp. 155–174. DOI: 10.17212/1994-6309-2024-26.1-155-174. (In Russian).

11. Lyubimyi N.S., Chetverikov B.S., Klyuev S.V., Zagorodniy N.A., Polshin A.A., Maltsev A.K., Bytsenko M.V. Investigation of the thermal loading during turning of a metal–composite system as a function of cutting speed, feed rate, and depth when machining a thin-walled 2 mm metal shell. *Obrabotka metallov (tekhnologiya, oborudovanie, instrumenty) = Metal Working and Material Science*, 2025, vol. 27, no. 4, pp. 131–147. DOI: 10.17212/1994-6309-2025-27.4-131-147. (In Russian).

12. *Lapshin V.P., Khristoforova V.V., Nosachev S.V.* Relationship of temperature and cutting force with tool wear and vibration in metal turning. *Obrabotka metallov (tekhnologiya, oborudovanie, instrumenty) = Metal Working and Material Science*, 2020, vol. 22, no. 3, pp. 44–58. DOI: 10.17212/1994-6309-2020-22.3-44-58. (In Russian).

13. Ślusarczyk Ł., Franczyk E. Estimation of temperature in the cutting area during orthogonal turning of grade 2 titanium. *The International Journal of Advanced Manufacturing Technology*, 2023, vol. 125, pp. 4485–4496. DOI: 10.1007/s00170-023-10877-5.

14. Ślusarczyk Ł. Experimental-analytical method for temperature determination in the cutting zone during orthogonal turning of GRADE 2 titanium alloy. *Materials*, 2021, vol. 14 (15), p. 4328. DOI: 10.3390/ma14154328.

15. Ranjbar S., Foorginejad A., Emam S.M., Ebadi M., Shiri K. Effects of cryogenic cooling on cutting temperature and surface roughness in turning of AA7075 aluminum alloy. *Scientific Reports*, 2026, vol. 16, p. 7914. DOI: 10.1038/s41598-026-39003-7.

16. Vornberger A., Picker T., Pötschke J., Herrmann M., Denkena B., Krödel A., Michaelis A. Influence of cemented carbide composition on cutting temperatures and corresponding hot hardnesses. *Materials*, 2020, vol. 13 (20), p. 4571. DOI: 10.3390/ma13204571.

17. Bohdanov O., Derbaba V., Dubrovskyi S., Ruban V., Nazarenco N. Study of cutting temperature during turningof high-hard cast irons. *Collection of Research Papers of the National Mining University*, 2023, vol. 75, pp. 44–54. DOI: 10.33271/crpnmu/75.044.

18. Sandhu N., Singh R., Singh N. Analysis of tool wear and cutting temperature in WS2-assisted MQL turning of H13 steel. *Discover Mechanical Engineering*, 2025, vol. 4, p. 55. DOI: 10.1007/s44245-025-00136-0.

19. Dubovska R., Majerik J., Baska I., Jambor J. Investigation of cutting temperature during AlCu3MgMnPb aluminium alloy turning. *Manufacturing Technology*, 2015, vol. 15 (5), pp. 796–801. DOI: 10.21062/ujep/x.2015/a/1213-2489/MT/15/5/796.

20. Kónya G., Takács J., Miskolczi I., Kovács Z.F. Investigation of the effects of machining parameters on cutting conditions during orthogonal turning of austenite stainless steel. *Production Engineering Archives*, 2024, vol. 30 (2), pp. 251–258. DOI: 10.30657/pea.2024.30.24.

21. Chaudhari R., Vora J.J., Parikh D.M. A review on applications of nitinol shape memory alloy. *Recent Advances in Mechanical Infrastructure. Lecture Notes in Intelligent Transportation and Infrastructure*. Singapore, Springer, 2021, pp. 123–132. DOI: 10.1007/978-981-33-4176-0_10.

22. Kul'chitskii A.A. Rezhimy rezaniya pri obrabotke nikel'-titanovykh splavov [Cutting modes for machining nickel-titanium alloys]. *Metalloobrabotka = Metalworking*, 2001, no. 3 (3), pp. 11–12.

23. Kazimirov D.Yu., Prokop'eva A.V., Astahov A.D., Medvedev O.A., Lushpey A.D. Uprochnenie poverkhnosti nitinola dlya povysheniya kachestva shlifovaniya [Surface hardening of nitinol for increased grinding quality]. *Aktual'nye problemy v mashinostroenii = Aktual Problems in Machine Building*, 2021, vol. 8, no. 3–4, pp. 25–29. (In Russian).

24. Albagachiev A.Yu., Khasyanova D.U. Osobennosti protsessa treniya pri dornovanii detalei iz nitinola [Friction in burnishing alloy parts with shape memory]. *Vestnik mashinostroeniya = Russian Engineering Research*, 2021, no. 5, pp. 40–43. DOI: 10.36652/0042-4633-2021-5-40-43. (In Russian).

25. Albagachiev A.Yu., Khasyanova D.U. Osobennosti formirovaniya i vysokotemperaturnoi obrabotki pustotelykh zagotovok pri izgotovlenii detalei iz splava s effektom pamyati formy [Production of hollow alloy blanks with shape memory effect]. *Vestnik mashinostroeniya = Russian Engineering Research*, 2019, no. 7, pp. 59–62. (In Russian).

26. Dutta S., Sarma D.K., Vora J., Chaudhari R., Bhowmik A., Samal P., Khanna S. A state-of-the-art review on micro-machining of nitinol shape memory alloys and optimization of process variables considering the future trends of research. *Journal of Manufacturing and Materials Processing*, 2025, vol. 9, p. 183. DOI: 10.3390/jmmp9060183.

27. Sureja D., Kumari S., Kumar R.S., Abhishek K., Saxena A., Abdullaev S.S. Experimental analysis and optimization of MQL turning of nitinol 56 alloy: a comparative study of grey, utility, and TOPSIS methods. *International Journal on Interactive Design and Manufacturing*, 2024, vol. 18, pp. 3427–3438. DOI: 10.1007/s12008-023-01621-0.

28. Naresh Ch., Sameer M.D., Bose P.S.Ch. Comparative analysis of RSM, ANN and ANFIS techniques in optimization of process parameters in laser assisted turning of NITINOL shape memory alloy. *Lasers in Manufacturing and Materials Processing*, 2024, vol. 11, pp. 371–401. DOI: 10.1007/s40516-024-00247-8.

29. Kumari S., Sureja D., Abhishek K., Kumar G. Utility function approach integrated with fuzzy for optimization in dry turning of nitinol 56. *Recent Advances in Materials and Manufacturing Science. ICRAM 2025. Lecture Notes in Mechanical Engineering.* Singapore, Springer, 2025, pp. 465–476. DOI: 10.1007/978-981-95-0063-5_36.

30. Kundiya R.R., Kadam M., Jadhav P., Pawade R. A review on high speed micro-milling of shape memory alloy (NiTinol): process and post perspective. *International Journal on Interactive Design and Manufacturing*, 2025, vol. 19, pp. 2337–2353. DOI: 10.1007/s12008-024-02153-x.

31. Naresh C., Bose P.S.C., Rao C.S.P. Artificial neural networks and adaptive neuro-fuzzy models for predicting WEDM machining responses of Nitinol alloy: comparative study. *SN Applied Sciences*, 2020, vol. 2 (2), pp. 1–23. DOI: 10.1007/s42452-020-2083-y.

32. Barbosa L.M.Q., França P.H.P., Fernandes G.H.N., Baldin V., Martins P.S., Machado Á.R. Using the chip-tool thermocouple method to measure the temperature in the milling of Inconel 718 under different lubri-cooling strategies. *The International Journal of Advanced Manufacturing Technology*, 2025, vol. 140, pp. 5435–5447. DOI: 10.1007/s00170-025-16568-7.

Conflicts of Interest

The authors declare no conflict of interest.